is a substantial difference in ionization at the relevant energy because of the density effect. We distinguish these two cases in Fig. 10.7. Fits were also made with functions of the form $a/(Z+b)^{\alpha}$, but α was essentially unity.

The transverse development of electromagnetic showers in different materials scales fairly accurately with the *Molière radius* R_M, given by [32,33]

$$R_M = X_0\, E_s/E_c\ , \tag{10.20}$$

where $E_s \approx 21$ MeV (see Table 10.1), and the Rossi definition of E_c is used.

In a material containing a weight fraction w_j of the element with critical energy E_{cj} and radiation length X_j, the Molière radius is given by

$$\frac{1}{R_M} = \frac{1}{E_s}\sum \frac{w_j\, E_{cj}}{X_j}\ . \tag{10.21}$$

For very high-energy photons, the total e^+e^- pair-production cross section is approximately

$$\sigma = \tfrac{7}{9}(A/X_0 N_A)\ , \tag{10.22}$$

where A is the atomic weight of the material and N_A is Avogadro's number. Equation Eq. (10.22) is accurate to within a few percent down to energies as low as 1 GeV. The cross section decreases at lower energies, as shown in Fig. 11.4 of this *Review.* As the energy decreases, a number of other processes become important, as is shown in Fig. 11.3 of this *Review.*

10.8. Electromagnetic cascades

When a high-energy electron or photon is incident on a thick absorber, it initiates an electromagnetic cascade as pair production and bremsstrahlung generate more electrons and photons with lower energy. The longitudinal development is governed by the high-energy part of the cascade, and therefore scales as the radiation length in the material. Electron energies eventually fall below the critical energy, and then dissipate their energy by ionization and excitation rather than by the generation of more shower particles. In describing shower behavior, it is therefore convenient to introduce the scale variables

$$t = x/X_0$$

$$y = E/E_c\ , \tag{10.23}$$

so that distance is measured in units of radiation length and energy in units of critical energy.

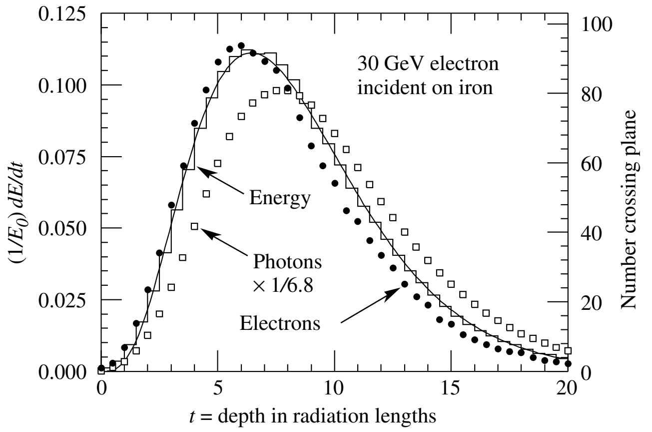

Figure 10.8: An EGS4 simulation of a 30 GeV electron-induced cascade in iron. The histogram shows fractional energy deposition per radiation length, and the curve is a gamma-function fit to the distribution. Circles indicate the number of electrons with total energy greater than 1.5 MeV crossing planes at $X_0/2$ intervals (scale on right) and the squares the number of photons with $E \geq 1.5$ MeV crossing the planes (scaled down to have same area as the electron distribution).

Longitudinal profiles for an EGS4 [8] simulation of a 30 GeV electron-induced cascade in iron are shown in Fig. 10.8. The number of particles crossing a plane (very close to Rossi's Π function [1]) is sensitive to the cutoff energy, here chosen as a total energy of 1.5 MeV for both electrons and photons. The electron number falls off more quickly than energy deposition. This is because, with increasing depth, a larger fraction of the cascade energy is carried by photons. Exactly what a calorimeter measures depends on the device, but it is not likely to be exactly any of the profiles shown. In gas counters it may be very close to the electron number, but in glass Čerenkov detectors and other devices with "thick" sensitive regions it is closer to the energy deposition (total track length). In such detectors the signal is proportional to the "detectable" track length T_d, which is in general less than the total track length T. Practical devices are sensitive to electrons with energy above some detection threshold E_d, and $T_d = T\,F(E_d/E_c)$. An analytic form for $F(E_d/E_c)$ obtained by Rossi [1] is given by Fabjan [34]; see also Amaldi [35].

The mean longitudinal profile of the energy deposition in an electromagnetic cascade is reasonably well described by a gamma distribution [36]:

$$\frac{dE}{dt} = E_0\, b\, \frac{(bt)^{a-1}e^{-bt}}{\Gamma(a)} \tag{10.24}$$

The maximum $t_{\rm max}$ occurs at $(a-1)/b$. We have made fits to shower profiles in elements ranging from carbon to uranium, at energies from 1 GeV to 100 GeV. The energy deposition profiles are well described by Eq. (10.24) with

$$t_{\rm max} = (a-1)/b = 1.0 \times (\ln y + C_j)\ , \qquad j = e, \gamma\ , \tag{10.25}$$

where $C_e = -0.5$ for electron-induced cascades and $C_\gamma = +0.5$ for photon-induced cascades. To use Eq. (10.24), one finds $(a-1)/b$ from Eq. (10.25) and Eq. (10.23), then finds a either by assuming $b \approx 0.5$ or by finding a more accurate value from Fig. 10.9. The results are very similar for the electron number profiles, but there is some dependence on the atomic number of the medium. A similar form for the electron number maximum was obtained by Rossi in the context of his "Approximation B," [1] (see Fabjan's review in Ref. 34), but with $C_e = -1.0$ and $C_\gamma = -0.5$; we regard this as superseded by the EGS4 result.

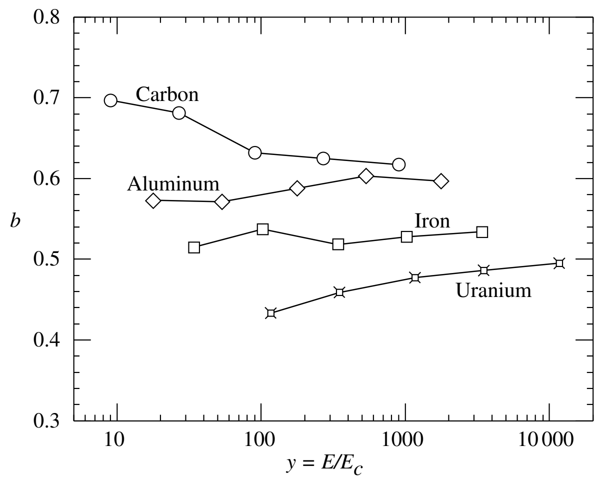

Figure 10.9: Fitted values of the scale factor b for energy deposition profiles obtained with EGS4 for a variety of elements for incident electrons with $1 \leq E_0 \leq 100$ GeV. Values obtained for incident photons are essentially the same.

The "shower length" $X_s = X_0/b$ is less conveniently parametrized, since b depends upon both Z and incident energy, as shown in Fig. 10.9. As a corollary of this Z dependence, the number of electrons crossing a plane near shower maximum is underestimated using Rossi's